High-silica mordenite as scaffold for phenylacetylene polymerization:
in situ High Pressure investigation

Giorgia Confalonieri[1], Marco Fabbiani[2], Rossella Arletti[1]*, Simona Quartieri[1], Francesco Di Renzo[3], Julien Haines[3], Gloria Tabacchi[4], Ettore Fois[4], Giovanna Vezzalini[1], Gianmario Martra[2] , Mario Santoro[5]

[1] Dipartimento di Scienze Chimiche e Geologiche, Università degli Studi di Modena e Reggio Emilia, via Campi 103, 41125 Modena, Italy

[2]Dipartimento di Scienze della Terra, Università degli Studi di Torino, via Valperga Caluso 35, 10125 Torino, Italy

[3]ICGM, CNRS, Université de Montpellier, ENSCM, Montpellier, France

[4]Dipartimento di Scienza ed Alta Tecnologia, Università dell'Insubria, and INSTM Via Valleggio 9, I-22100 Como, Italy

Via Valleggio 5, Como, Italy

[5]Istituto Nazionale di Ottica, CNR-INO, and European Laboratory for Non Linear Spectroscopy (LENS), 50019 Sesto Fiorentino, Italy

*Corresponding author, e-mail: rossella.arletti@unimore.it

Abstract

The joint use of high pressure and regular void-space architectures is a promising route to obtain new nanomaterials with unique properties. We explore herein the pressure-driven injection of aromatic guest species inside zeolite mordenite. Monomeric phenylacetylene (PhA), used as pressure transmitting medium, was inserted in high-silica mordenite at high pressure conditions. In-situ X-ray powder diffraction and IR spectroscopy analyses show that the combined action of high pressure, temperature and zeolite pores accomplish the intrusion of phenylacetylene and its conversion to oligomeric species exhibiting a greater degree of conjugation with respect to the starting monomer. This study may open a new path for the realization of composite materials with

interesting optoelectronic properties via pressure-driven intrusion and polymerization of aromatic molecules inside zeolite frameworks.

Keyword: pure-silica mordenite, high-pressure, hydrocarbon-polymerization

1. Introduction

Zeolite materials, thanks to their unique properties, related to their composition and pore topology, are of paramount importance in many technological processes, such as catalysis, adsorption, separation and ion exchange [1-4].

Due to their structure, zeolites pores can be filled by suitable guest molecules (organic or inorganic) and cations, more or less able to diffuse in the pores [5,6]. Their level of hydrophilicity/hydrophobicity, thus the fate of the competitive adsorption of water *vs* other molecules can be modulated by varying their SiO_2/Al_2O_3 ratio. Thanks to their void architecture, zeolites can also be adopted as "moulds" for creating regular arrays of molecules to develop functional materials [6], such as: i) semiconductor quantum dots and wires [7]; ii) artificial antenna systems constituted by wires of organic dyes running along the zeolite mono-dimensional channel system [8-9]; (iii) luminescent materials obtained by the insertion of lanthanide arrays in the zeolite channels [10]; (iv) effect pigments [11]. Moreover, by operating at high pressure (HP) conditions, novel supramolecular arrangements can be produced by the zeolite "mould" [12-13].

Once the pores are filled, reactions can be initiated and controlled inside the zeolite's cavities. It has been demonstrated that HP is an ideal tool for implementing chemical reactions induced by purely mechanical methods, by tuning the intermolecular/interatomic distances and causing a rearrangement of chemical bonds. The nano-confinement, deriving from the combination of HP with the geometrical constraints imposed by the zeolitic framework, has proven to be effective in driving the formation of polymers with desired dimensionality, such as polyethylene,[14] polyacetylene [15] and polycarbonyl [16]. Preparing isolated, self-standing, densely packed polymers, protected by a hydrophobic matrix, is very challenging via conventional protocols [17-18].

Here, we exploit the porous template effectiveness of zeolites to investigate for the first time the reactivity, under HP conditions, of a molecule containing an aromatic moiety. In particular, we focalize our efforts on the incorporation of phenylacetylene (PhA) in a high-silica phase of zeolite mordenite (HS-MOR). Our choice is due to the fact that, in most of the zeolite-based devices, guest species are generally characterized by high optical absorbance properties [7-11]. Hence, the presence of an aromatic ring in PhA might help to impart interesting optoelectronic properties to the zeolite-based composite material, which might be exploited in new devices for practical applications - like, for example, gas sensing [19].

By injecting monomeric PhA molecules as pressure transmitting medium inside a high-silica mordenite and following their behaviour under HP, in this work we provide evidence of the nearly-complete disappearance of phenyl acetylene in favour of the formation of encapsulated carbocationic poly-PhA oligomers.

2. Materials and Methods

2.1 Materials

A high silica mordenite (purchased from the Tosoh Corporation – code HSZ-690HOA Tosoh – in its protonated form, Si/Al ~ 200, *i.e.* ca. 0.5 Al per unit cell, HS-MOR hereafter) was selected as the host material, considering the following specific needs: i) its pore dimensions allow the penetration of the molecules of interest; ii) the framework has a mono-dimensional channel system, suitable to promote the synthesis of 1D isolated polymer chains; iii) the connection among the channels will allow the gas circulation. This latter is a crucial point for the realization of a gas sensing device: an effective gas circulation requires mono-dimensional non-intersecting - but communicating - parallel channels with different diameter, one larger channel in which the polymerization will be realized, and one smaller channel for gas diffusion. The contact between the parallel channels is ensured in MOR topology by sufficiently large windows between them.

Mordenite: Mordenite (framework type MOR [20], space group *C*mcm,) crystal structure exhibits a 1D channel system characterized by two parallel channels running along the c axis: a large almost circular 12MR channels (''free diameters'' 6.5 Å x 7.0 Å) and a strongly elliptic 8MR channels (''free diameters'' 2.6 Å x 5.7 Å). These channels are interconnected along the [010] direction through side pockets delimited by two 8MR apertures that, in turn, form a sinusoidal channel (''free diameters'' 3.4 Å x 4.8 Å) running along the b axis [21]. As a whole, two 12MR and two 8MR are present in a single unit cell.

The pristine material has been fully characterized and previously used in a number of studies [22-24]. A representation of MOR framework and structural data of the pristine HS-MOR here used are reported in Figure 1 and in Table 1, respectively.
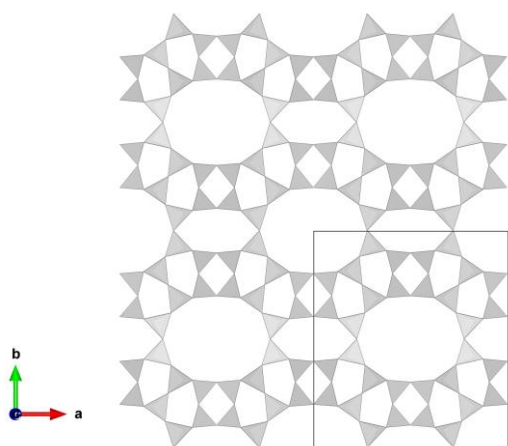
Figure 1. MOR framework structure viewed along the [001] direction. Unit cell is drawn.

Table 1: Data relative to the pristine HS-MOR used for phenylacetylene loading. *taken from the structural refinement reported in reference [23].

HS-MOR	
SiO$_2$/Al$_2$O$_3$	~200
Space group	*C*mcm
a (Å)	18.0519(8)
b (Å)	20.2061(8)
c (Å)	7.4506(3)
V (Å^3)	2717.7(2)
H$_2$O molecules p.u.c.* (material exposed to air)	3.6

98%pure *Phenylacetylene:* Pure phenylacetylene (PhA hereafter) purchased by Sigma Aldrich.

2.2 Pore dimensions evaluation

Textural properties were evaluated by N$_2$ adsorption at 77 K in a vacuum-improved Micromeritics Tristar apparatus after outgassing at 250°C. Mesopore volume was measured by the αS method and mesopore size distribution was evaluated by the DFT method.

2.3 High pressure experiments

To unravel the formation of PhA polymer inside HS-MOR and its stability inside zeolite channels, the guest-guest and host-guest interactions were investigated by *in situ* HP X-ray powder diffraction experiments (HP-XRPD) and HP Infrared Spectroscopy (HP-IR) experiments.

2.3.1 HP-XRPD

Some preliminary patterns were collected on a conventional diffractometer (Mo Kα Radiation), but data quality allows only qualitative considerations on pore filling (see below), so all the HP-XRPD experiments were collected at synchrotron facilities

HP - XRPD experiments were performed at the beamline BM01, ESRF (European Synchrotron Radiation Facility, Grenoble France) using a modified Merrill–Basset Diamond Anvil Cell [25]. Pressure was calibrated using the ruby fluorescence method [26] on a nonlinear hydrostatic pressure scale (the estimated error is 0.05 GPa) [27]. Pure PhA was used as penetrating Pressure Transmitting Medium (PTM). The experiments were performed in Debye Scherrer geometry with a fixed wavelength of 0.68202 Å. Diffraction intensities were collected on a Pilatus Dectris detector (with pixel dimensions of 172 μm x 172 μm) positioned at a fixed distance of 238.98 mm from the sample. Pressure was increased up to 1.34 GPa and then the pressurized DAC was kept in oven at 150°C for 5 hours. Then a diffraction pattern was collected. Diffraction images were integrated and treated obtaining one-dimensional patterns using the Dioptas program [28].

Structure refinement was performed on the pattern collected at 0.40 GPa in the *C*mcm space group using the GSAS package [29] with the EXPGUI [30] interface, starting from the framework atomic coordinates reported in [23]. The extra-framework sites (oxygen atoms of water and PhA molecules) were localized through the inspection of the difference Fourier map. The background curve was fitted using a Chebyshev polynomial with 24 coefficients. The pseudo-Voigt profile function proposed by Thompson [31] was used with a peak intensity cut-off set to 0.1% of the strongest peak. Soft-restraints were applied to the T–O (1.60 Å) and C-C distances (1.50(2), 1.40(2) and 1.25(2) Å for the single, double and triple bonds respectively); the weight was gradually decreased, after the initial stages of refinement, up to a final weight of 50. The isotropic displacement parameters were constrained in the following way: a value for all the tetrahedral cations, a second value for all the framework oxygen atoms, a third value for the carbon atoms and a fourth for water oxygen atoms. Details of the structural refinement are reported in Table 2. Atomic coordinates, occupancy factors, and thermal parameters, along with selected bond distances (Å) are reported as Supporting Information (Tables 1S and 2S, respectively). The final observed and calculated powder patterns for HS-MOR PhA at 0.40 GPa are provided in Figures S1.

Table 2: Structural refinement parameters of HS-MOR compressed in PhA at 0.40 GPa.

	0.40 GPa
Space group	Cmcm

|	
a (Å)	18.119(1)
b (Å)	20.235(2)
c (Å)	7.4619(6)
$V(Å^3)$	2735.8(3)
R_{wp} (%)	0.1031
R_p (%)	0.007
R_F^2 (%)	0.10
N_{obs}	947
N_{var}	71

2.3.2 HP-IR

For investigating HS-MOR/PhA mixtures at high pressures by IR absorption spectroscopy, we used membrane DACs with a diamond culet diameter of 600 μm and equipped with stainless steel gaskets. Typical sample diameter and thickness were 200 μm and about 50 μm, respectively. The cell was loaded with pure phenylacetylene as PTM. A ruby chip was also put in the sample chamber for pressure measurements [27]. After closing the cell, the liquid hydrocarbon filled both the pores of the zeolite (confined PhA), as testified by changes in the relative intensity of X-ray diffraction Bragg peaks of HS-MOR, and the residual empty space between the grains of mordenite (bulk PhA). High pressure, IR spectra on HS-MOR/PhA were measured with resolution of 1.0 cm^{-1}, using a Bruker IFS-120 HR Fourier transform infrared spectrometer equipped with an optical beam condenser based on ellipsoidal mirrors [32]. The IR spot diameter is typically larger than the sample diameter and, consequently, the gained information on chemical structure corresponds to the spatial average of this structure over the whole sample size.

3. Results

3.1 Surface area and pores dimensions of pristine HS-MOR

To obtain information on the pore dimension distribution, HS-MOR sample was characterized by N_2 adsorption. The N_2 sorption (Figure 2) follows a type 1 isotherm, typical of a microporous solid, with some specific features. The onset of adsorption at low pressure is less sharp than expected in a purely microporous solid. The presence of a continuous transition between microporosity (diameter lower than 2 nm) and small mesoporosity has to be considered in the evaluation of the micropore volume by comparison methods. The αS plot cannot be linearized below αS=1. As a

consequence, the volume of small pores evaluated by this method, 0.22 cm^3 g^{-1}, is not limited to micropores, but it includes all pores with diameter smaller than 4 nm. A DFT analysis of mesopore size distribution indicates a pore volume of 0.021 cm^3 g^{-1} distributed in the size range 2-4 nm. If this volume is subtracted from the αS data, the true micropore volume can be evaluated at 0.20 cm^{3}g^{-1}. This continuous transition between micropores and mesopores is expected in a dealuminated commercial sample, as the dealumination procedure is well known to induce defects and to open side communications between side pockets of mordenite. Dealumination methods can also open mesopores with larger size. The total mesopore volume of the sample between 2 and 60 nm diameter is 0.061 cm^3 gr^{-1}, of which 0.037 are widely distributed in the diameter range between 6 and 60 nm.
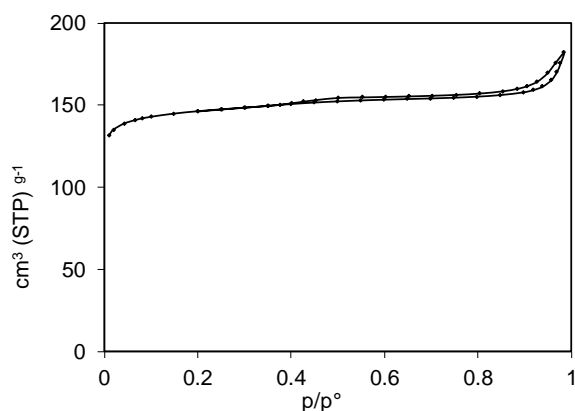

Figure 2 Adsorption-desorption N$_2$ isotherm at 77 K.

3.2 X-ray powder diffraction experiments

To explore the possibility of injecting PhA inside the HS-MOR pores, a preliminary qualitative test was performed with conventional (Mo Kα source) X-Ray powder diffraction (XRPD) in Diamond Anvil Cell (DAC). Figure 3 reports the patterns collected before and after the contact of the powder with liquid PhA.
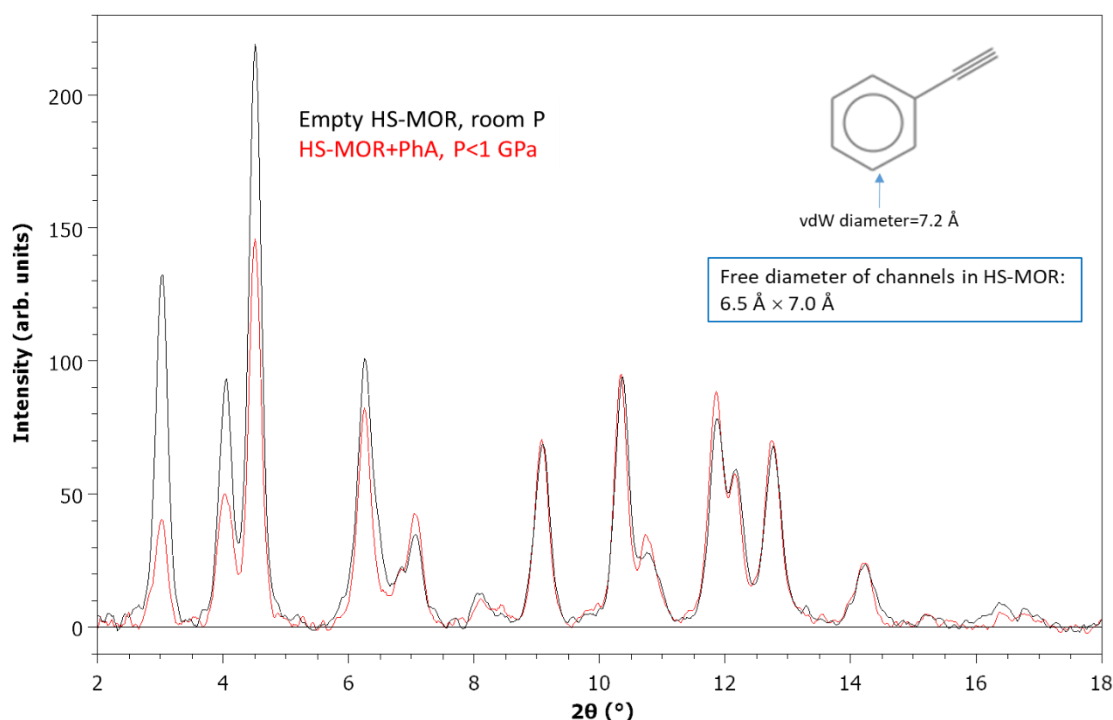
Figure 3: HS-MOR XRPD patterns measured in a DAC before (black) and after loading liquid PhA (red). A molybdenum X-ray micro-source (λ=0.71073 Å) has been used. The strong Compton background from diamonds and the broad diffuse diffraction pattern from liquid PhA have been subtracted. The two patterns have been normalized for the same intensity at 9.1°-10.3°.

It is evident that the simple contact between HS-MOR and PhA under very mild pressure conditions (obtained by simply closing the DAC) induces strong changes in the intensity of the low-angle diffraction peaks. Being these peaks strongly influenced by the extraframework content, we can assume that some PhA molecules are intruded in HS-MOR microporosity. This result is not obvious since the Van der Waals diameter of a PhA molecule is 7.2 Å, whereas the nominal 12MR channel diameter of MOR is 6.5x7.0 Å. However, the penetration of species slightly larger than the pores dimension in zeolites at low pressure, or even at ambient pressure (P_{amb}) conditions, has been already demonstrated in a number of studies which pinpointed the key role of both zeolite-flexibility and guest molecule flexibility in the insertion process [33-37]. In particular, also guest species possessing aromatic rings show a surprisingly high flexibility of the molecular structure, which allows for both the encapsulation and the diffusion of these species inside the zeolite channels [38].

An accurate X-ray powder diffraction structural analysis was performed at 0.40 GPa. At higher pressures, the bad quality of the data lead to unrealistic distances and did not allow a reliable structural refinement. The refinement at 0.40 GPa indicates that the compression of HS-MOR by PhA leads to an expansion of the unit cell along all the three axes, in comparison to the values

measured at ambient pressure (Table 1 and Table 2). In particular, the *a* parameter shows an increase of about 0.30 %, while *b* and *c* expand by 0.14 and 0.15 %, respectively. This anisotropic behavior of the cell parameters is related to the intrusion and the consequent arrangement of the extraframework molecules in the porosities.
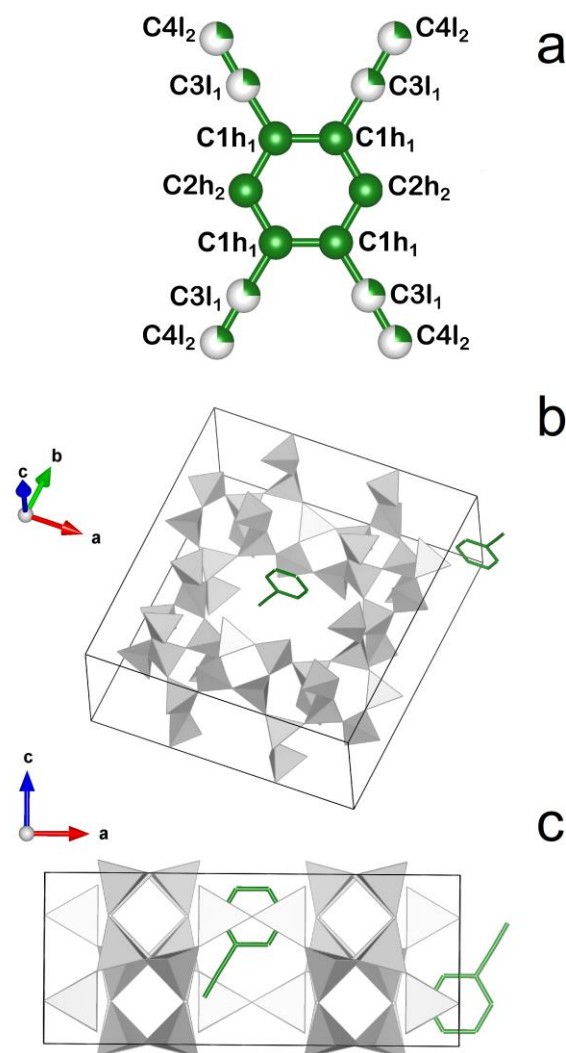

Figure 4: a) Phenylacetylene molecule showing the labels used for the carbon sites. b and c) Structural model of HS-MOR compressed in phenylacetylene at 0.40 GPa (water molecules are omitted for clarity). The two figures show only the average positions actually occupied rather than all the partially occupied symmetrically equivalent positions.

As a whole, 2 molecules of PhA per unit cell, distributed over 4 equivalent sites, were located in the 12MR channels (Tables 1S and 2S). The molecules, on average, are parallel and lie near the center of the channel on two equivalent planes parallel and close to the (020) plane. This induces a larger increase of the *a* lattice parameter. Despite PhA molecules can be sited over 4 equivalent sites (two in each 12MR channel), the too short distance (1.8300(1) Å) between two carbon-cycles belonging to two different molecules suggests the distribution of the two phenylacetylene

molecules into two different channels. For each molecule, phenyl sites ($C1h_1$ and $C2h_2$, see Figure 4a) are uniquely located, while the position of the C≡CH acetylenic moiety has four possible crystallographically equivalent orientations ($C3l_1$ and $C4l_2$ carbon atoms in Figure 4). Figures 4b and 4c show the average refined structure, reporting two possible PhA molecule configurations inside the mordenite microporosities. Along with the PhA molecules, 3.2 H_2O molecules were localized in the side-pockets between the 12 and 8MR channels. From the structural model obtained, it is possible to conclude that PhA monomers at 0.40 GPa have very week interaction with the zeolite framework.

As shown in Figure 5, upon pressure increase, the relative intensity of the diffraction peaks changes, indicating further intrusion of phenylacetylene. Unfortunately, the high disorder affecting the extraframework species does not allow to localize the PhA molecules in the channels. After the compression at 1.34 GPa, the DAC was kept in oven at 150°C for 5 hours (high temperature treatment, HT hereafter). Upon heating, the pressure reached 2.58 GPa, whereas in the room temperature (r.t.) quenched sample, the pressure returned to the pristine value of 1.35 GPa. The powder diffraction pattern collected after the HP-HT treatment shows new slight differences in the peak intensity and in their ratio with respect to the pattern collected at r.t. (Figure 5). Due to the strong peak broadening, no further consideration can be made on the evolution of the cell parameters. Indeed, the cell parameters values at 1.34 GPa ($a = 18.05(8)$ Å, $b = 18.0(1)$ Å, $c = 7.40(5)$ Å, $V = 2670(28)$ Å^3) and after thermal treatment ($a = 18.1(2)$ Å, $b = 20.0(3)$ Å, $c = 7.4(1)$ Å, $V = 2675(56)$ Å^3) are affected by very high standard deviations, which do not allow to appreciate any differences between the two sets.
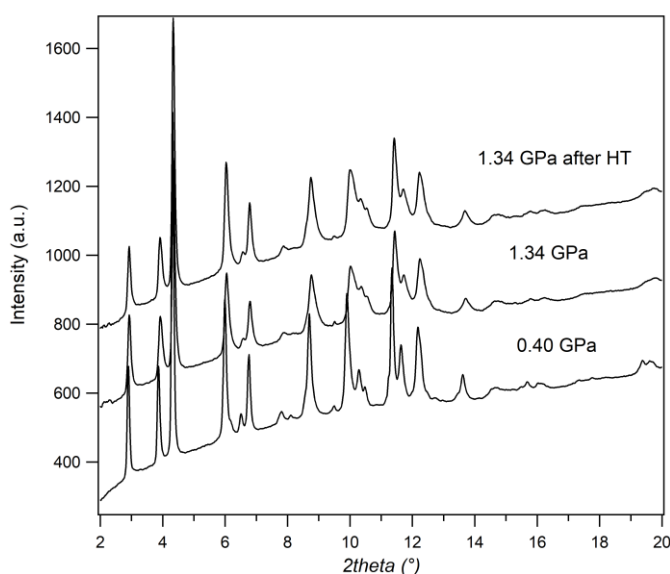
Figure 5: Diffraction patterns of HS-MOR compressed in phenylacetylene at 0.40 GPa, 1.34 GPa and at 1.34 GPa after HT treatment.

3.3 Infrared spectroscopy Investigation

In Figure 6, we report selected high pressure IR absorption spectra of HS-MOR/PhA mixtures and of pure PhA, measured along similar P-T paths.

The IR investigation on the high pressure - high temperature polymerization of pure PhA here serves as a reference background to interpret analogous results on HS-MOR/PhA mixtures. Pure PhA solidifies above 1.10 GPa forming a molecular solid and it does not polymerize below 8.00 GPa at room temperature [39]. On the other hand, here we found that high temperature severely enhances the high pressure polymerization of PhA. Indeed, solid PhA at 2.00 GPa is chemically stable (Figure 6, top spectra) over days at least, whereas heating the sample to 150 °C at nearly the same pressure for 18 h results in almost the 100% polymerization of the starting monomer. This occurs likely because the sample is melted and the mass diffusivity and chemical reactivity are increased. The material recovered after the HP-HT treatment is polyPhA, a red solid material. This polymer is made of a skeletal conjugated carbon chain, where conjugation relates to the red color, while the phenyl groups are chemically unaffected by the polymerization reaction [39]. Monomeric and polymeric PhA exhibit IR peaks at rather similar frequencies in the 1400-1650 cm^{-1} range, although relative intensities and line-shapes of those peaks substantially differ for the two species. The C-H stretching peaks at 2800-3400 cm^{-1} are a direct easy probe for the carbon coordination changes in going form the monomer to the polymer. Indeed, the very strong ≡C(sp)-H stretching peak of the monomer at 3300 cm^{-1} is drastically reduced in intensity during the thermal treatment and it is hardly visible in the polymer, showing that the polymerization is almost complete. This is accompanied by a substantial intensity increase in the 3000–3150 cm^{-1} frequency range where C-H stretching vibrations from sp^2 carbon are typically found, and we interpret this increase mostly with the formation of the conjugated -C=C- skeleton system of polyPhA. The C-H stretching IR peak of this skeleton partially overlaps to those of the aromatic phenyl groups. Then, an intensity increase in the 2800-3000 cm^{-1} region is also observed during the thermal treatment, due to C-H stretching modes of saturated sp^3 C defects, which always form together with the conjugated polymer.
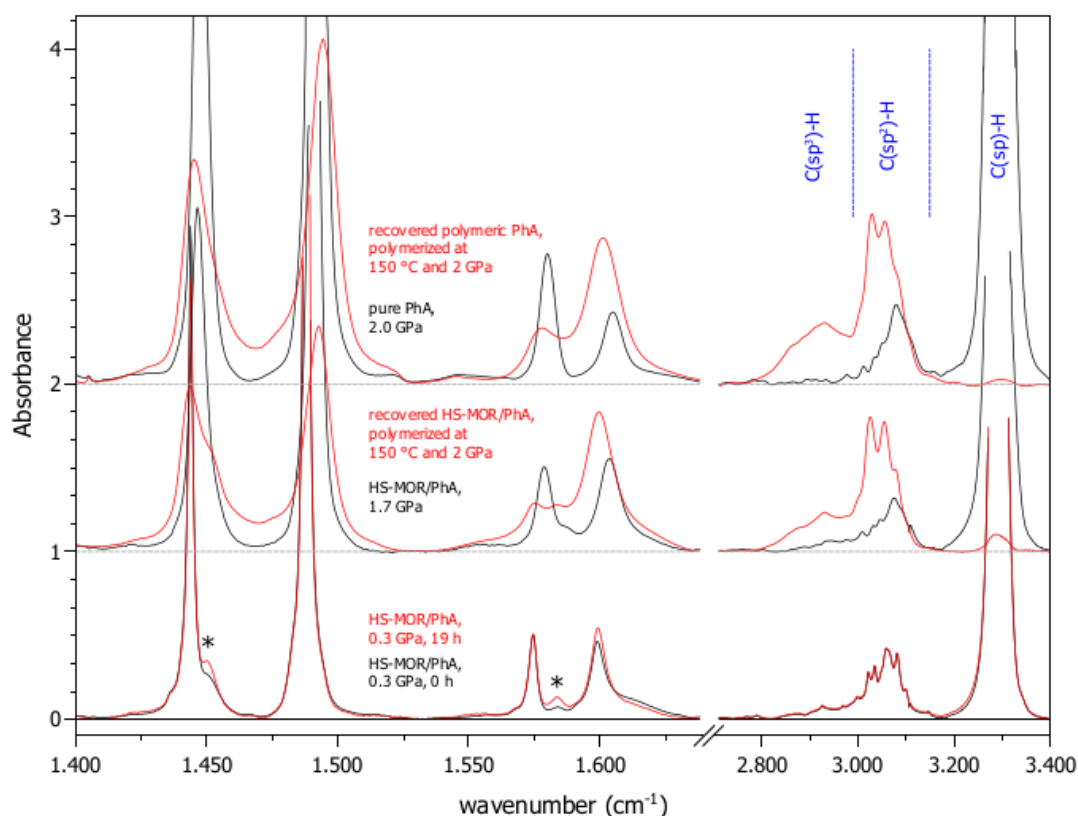
Figure 6: Selected, high pressure IR absorption spectra of HS-MOR/PhA mixtures and of pure PhA. Bottom: spectra of a HS-MOR/PhA sample at 0.30 GPa, freshly loaded in DAC (black) and after 19 h (red). Stars indicate short oligomers formed as a function of time. Middle: spectra of the same sample at 1.70 GPa (black) and of the recovered sample at ambient conditions (red), after polymerization of PhA obtained in about 13 h at 150 °C and 2.00 GPa. Top: spectra of a pure PhA sample at 2.00 GPa (black) and of the recovered sample at ambient conditions (red), after polymerization obtained in about 18 h at 150 °C and 2.00 GPa. Spectral intervals for peaks due C(sp^3)−H, C(sp^2)−H and C(sp)−H stretching modes are also labeled in blue. An absorption spectrum of pure HS-MOR measured at ambient pressure in DAC has been subtracted from all the spectra of HS-MOR/PhA.

Figure 6 (bottom) shows selected IR spectra of a HS-MOR/PhA sample sealed at 0.30 GPa, a pressure where PhA is a liquid monomer. Spectra measured over a time interval of about 19 h show the slow formation of new peaks, labeled by asterisks in the figure, which belong neither to monomeric nor to polymeric PhA. These peaks can be assigned to short carbo-cationic oligomers probably formed as a result of the catalytic action of mordenite. In fact, these peaks do not appear in the pure PhA sample. Anyway, the catalyzed reaction of PhA is at a very initial stage after 19 h and the vast majority of initial monomeric PhA is still present, as shown by the strong, always saturating C(sp)-H stretching peak of monomeric PhA at 3300 cm^{-1}. The sample was then compressed at 1.70 GPa (Figure 6, middle, black spectrum), above the solidification pressure of PhA, and the polymerization stopped entirely over a probing time interval of about 24 h, probably because of the solidification related drop of mass diffusivity, which hinders the reactivity of the monomer. Finally, the HS-MOR/PhA sample was brought to the same P-T conditions of pure PhA (i.e. 150 °C at 2.00 GPa, for

13

13 h) (Figure 6, middle, red spectrum) and the PhA component of the mixture polymerized almost entirely, probably because of the melting related increase of mass diffusivity of PhA, as discussed above. The IR spectrum of the mixed recovered sample, whose picture is reported in Figure 7, is rather similar to that of polymeric pure PhA.
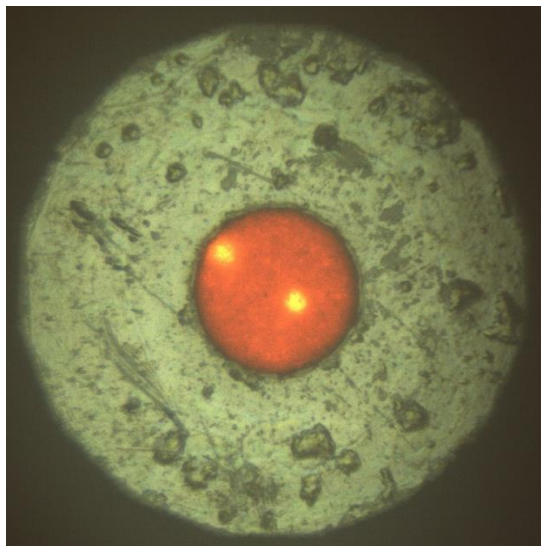
Figure7. Picture of HS-MOR/PhA (red sample in the center of the metallic gasket) at almost ambient pressure after the high P-T polymerization of PhA described in the text. The orange/yellow chips within the sample are the rubies used for measuring pressure. The gasket diameter is 600 ⍰m and the sample is illuminated both by transmitted and reflected light.

4. Discussion and Conclusion

The experiments performed indicated that, despite the larger dimensions with respect to the zeolite pore openings, phenylacetylene molecules can indeed enter the mordenite pores even at very low pressure (almost P_{amb}). The increase of the pressure favors the further penetration of the molecules in the microporosity and, as shown by the X-ray diffraction data, it is possible to conclude that at 0.40 GPa, on average, two phenylacetylene molecules are hosted in each mordenite unit cell. This number is lower with respect to that estimated on the basis of the steric hindrance of the guest molecules. Such a result can be understood by noting that the diffusion of species of size comparable to the pores openings – such as PhA in HS-MOR - is slowed down by the so-called "traffic jam" effect – *i.e.* the crowding of molecules close to zeolite pore entrances [37]. This effect may be overcome by HP: indeed, further penetration of PhA molecules occurs upon pressure increase, as witnessed by the changes in the relative intensities of X-ray diffraction peaks. However, probably due to the statistical disorder in the pores at higher pressure (and evidenced by the worsening of the diffraction pattern with compression) it has not been possible to quantify the maximum number of molecules at the highest investigated pressure.

In the absence of a detailed structural investigation, spectroscopic data gave important clues to unravel the evolution of the system at higher pressure. In fact, IR spectra suggest a slow oligomerization reaction, observed at 0.30 GPa, forming short carbo-cationic oligomers. These species do not form in the pure PhA sample at the same conditions, so they should result from the interaction with mordenite that catalyzes the reaction. The limited spatial resolution of the experiment did not allow to analyze specifically the PhA in contact/hosted with/in the mordenite framework; on the other hand, from the IR spectra, we clearly found that the vast majority of initial monomeric PhA is still present at 0.30 GPa. Oligomer molecules were not detected by HP-XRPD, firstly because these oligomers form disordered arrays, and diffraction can offer only average structures, and secondly because the oligomerization kinetics is much slower (hours) than the data collection time (minutes).

Once the applied pressure reaches that of PhA solidification (~1.10 GPa), the molecular system freezes and in order to observe further evolution of the system higher temperature is needed: once the PhA molecular solid formed in the gasket melts upon heating, it is possible to observe further reactivity and the complete polymerization of PhA into poly-phenylacetylene. Once again it is not possible to distinguish between the IR signals coming from the zeolites+PhA (polyPhA) mixture and from the pure polyPhA present inter – grains, even if it is possible to conclude the PhA is completely consumed in favor to the polymer.

Interestingly, despite the choice of a zeolite characterized by a mono-dimensional channel system, the IR spectra measured on the polymerized samples indicated the presence of somewhat branched, conjugated polymers, rather than ideally linear, fully conjugated polymers. This is clearly due to the presence of a certain degree of mesopores in the starting zeolites: the de-alumination procedure, aimed at the obtainment of a high silica phase, is well known to induce strong defectivity, leading to a non-perfectly mono dimensional structure. Anyway, it is worth noting that at least part of the polyPhA we observe through IR – i.e portions of conjugated oligomers- can also be allocated within the mesopores of HS-MOR. Hence, we can conclude that the combined action of HP and space confinement has produced a zeolite-based composite material in which the guest species has a degree of conjugation greater than the starting monomer, as witnessed by the red color of the recovered sample. This evidence holds promises for the realization of new materials with intriguing optoelectronic properties via pressure-driven polymerization of aromatic molecules inside zeolite cages. Further studies will be aimed to obtain a linear conjugated polymer in a non-defective framework characterized by monodimensional channel system.

Acknowledgement

[1] B.M. Weckhuysen, J.H. Yu, Chem. Soc. Rev., 44 (2015) 7022-7024.

[2] J. Čejka, A. Corma, S. Zones, Zeolite and Catalysis. Synthesis, Reactions and Applications, Wyley-YCH, Weinheim, 2010.

[3] Xu R., Pang W. , Yu J. , Huo Q., Chen J. , Chemistry of Zeolites and Related Porous Materials: Synthesis and Structure, John Wiley & Sons (Asia) Pte Ltd., 2007.

[4] R.P. Townsend, E.N. Coker, Ion exchange in zeolites, in: H. van Bekkum, E.M. Flanigen, P.A. Jacobs, J.C. Jansen (Eds.) Introduction to Zeolite Science and Practice, Amsterdam ; New York: Elsevier 2011.

[5] G.D. Gatta, P. Lotti, G. Tabacchi, Phys. Chem. Miner., 45 (2018) 115-138.

[6] G. Tabacchi, Chemphyschem, 19 (2018) 1249-1297.

[7] N.C. Jeong, H.S. Kim, K.B. Yoon, Langmuir, 21 (2005) 6038-6047.

[8] R. Garcia, V. Martinez-Martinez, R.S. Llano, I. Lopez-Arbeloa, J. Perez-Pariente, J. Phys. Chem. C, 117 (2013) 24063-24070.

[9] L. Gigli, R. Arletti, G. Tabacchi, E. Fois, J.G. Vitillo, G. Martra, G. Agostini, S. Quartieri, G. Vezzalini, J. Phys. Chem. C, 118 (2014) 15732-15743.

[10] H. Maas, A. Currao, G. Calzaferri, Angew. Chem. Int. Ed., 41 (2002) 2495-2497.

[11] P. Woodtli, S. Giger, P. Muller, L. Sagesser, N. Zucchetto, M.J. Reber, A. Ecker, D. Bruhwiler, Dyes Pigments, 149 (2018) 456-461.

[12] R. Arletti, E. Fois, L. Gigli, G. Vezzalini, S. Quartieri, G. Tabacchi, Angew. Chem. Int. Ed., 56 (2017) 2105-2109.

[13] G. Confalonieri, S. Quartieri, G. Vezzalini, G. Tabacchi, E. Fois, T.J. Daou, R. Arletti, Microporous and Mesoporous Mater., 284 (2019) 161-169.

[14] M. Santoro, F.A. Gorelli, R. Bini, J. Haines, A. van der Lee, Nature Communications, 4 (2013) 3761-3767.

[15] D. Scelta, M. Ceppatelli, M. Santoro, R. Bini, F.A. Gorelli, A. Perucchi, M. Mezouar, A. van der Lee, J. Haines, Chem. Mater., 26 (2014) 2249-2255.

[16] M. Santoro, D. Scelta, K. Dziubek, M. Ceppatelli, F.A. Gorelli, R. Bini, G. Garbarino, J.M. Thibaud, F. Di Renzo, O. Cambon, P. Hermet, J. Rouquette, A. van der Lee, J. Haines, Chem. Mater., 28 (2016) 4065-4071.

[17] H. Bassler, Nat .Phys., 2 (2006) 15-16.

[18] D.J. Cardin, Adv. Mater., 14 (2002) 553-563.

[19] P.T. Moseley, D.E. Williams, Techniques and Mechanism in Gas Sensing, Adam Hilger, Bristol, UK, 1991.

[20] C. Baerlocher, L.B. McCusker, D.H. Olson, Atlas of zeolite framework types, 6th ed., Elsevier, Amsterdam, The Netherlands, 2007.

[21] W.M. Meier, Z. Kristallogr. Cryst. Mater., 115 (1961) 439-450.

[22] A. Martucci, L. Pasti, M. Nassi, A. Alberti, R. Arletti, R. Bagatin, R. Vignola, R. Sticca, Microporous and Mesoporous Mater., 151 (2012) 358-367.

[23] R. Arletti, L. Leardini, G. Vezzalini, S. Quartieri, L. Gigli, M. Santoro, J. Haines, J. Rouquette, L. Konczewicz, Phys. Chem. Chem. Phys., 17 (2015) 24262-24274.

[24] R. Fantini, R. Arletti, S. Quartieri, M. Fabbiani, S. Morandi, G. Martra, F. Di Renzo, G. Vezzalini, Microporous and Mesoporous Mater., 294 (2019).

[25] R. Miletich, D.R. Allan, W.F. Kush, High Temperature and High-Pressure Crystal Chemistry, in: R.M. Hazen, R.T. Downs (Eds.) Reviews in Mineralogy and Geochemistry Mineralogical Society of America and Geochemical Society Washington, USA, 2000, pp. 445-519.

[26] R.A. Forman, G.J. Piermarini, J.D. Barnett, S. Block, Science, 176 (1972) 284-285.

[27] Mao, K. H, J. Xu, P.M. Bell, J. Geophys. Res., 91 (1986) 4673.

[28] C. Prescher, V.B. Prakapenka, High Pressure Res., 35 (2015) 223-230.

[29] Larson, C. A, R.B. Von Dreele, Los Alamos National Laboratory Report, (1994).

[30] B.H. Toby, J. Appl. Crystallogr., 34 (2001) 210-213.

[31] P. Thompson, D.E. Cox, J.B. Hastings, J. Appl. Crystallogr., 20 (1987) 79-83.

[32] F.A. Gorelli, L. Ulivi, M. Santoro, R. Bini, Phys. Rev. Lett., 83 (1999) 4093-4096.

[33] G. Calzaferri, S. Huber, H. Maas, C. Minkowski, Angew. Chem. Int. Ed., 42 (2003) 3732-3758.

[34] G. Tabacchi, E. Fois, G. Calzaferri, Angew. Chem. Int. Ed., 54 (2015) 11112-11116.

[35] G. Tabacchi, G. Calzaferri, E. Fois, Chem. Commun., 52 (2016) 11195-11198.

[36] L. Gigli, R. Arletti, G. Tabacchi, M. Fabbiani, J.G. Vitillo, G. Martra, A. Devaux, I. Miletto, S. Quartieri, G. Calzaferri, E. Fois, J. Phys. Chem. C, 122 (2018) 3401-3418.

[37] M. Busby, A. Devaux, C. Blum, V. Subramaniam, G. Calzaferri, L. De Cola, J. Phys. Chem. C, 115 (2011) 5974-5988.

[38] E. Fois, G. Tabacchi, G. Calzaferri, J. Phys. Chem. C, 116 (2012) 16784-16799.

[39] M. Santoro, L. Ciabini, R. Bini, V. Schettino, J. Raman Spectr., 34 (2003) 557-566.